

Proteome analysis of recombinant *Escherichia coli* producing human glucagon-like peptide-1[☆]

Dae-Hee Lee^a, Sung-Gun Kim^b, Yong-Cheol Park^c,
Soo-Wan Nam^d, Kelvin H. Lee^e, Jin-Ho Seo^{a,b,*}

^a Department of Agricultural Biotechnology and The BioMAX Institute, Seoul National University, Seoul 151-921, South Korea

^b Interdisciplinary Program for Biochemical Engineering and Biotechnology, Seoul National University, Seoul 151-744, South Korea

^c Center for Agricultural Biomaterials, Seoul National University, Seoul 151-921, South Korea

^d Department of Biotechnology and Bioengineering, Dong-Eui University, Busan 614-714, South Korea

^e School of Chemical and Biomolecular Engineering, Cornell University, Ithaca, NY 14853, USA

Received 30 May 2006; accepted 8 September 2006

Available online 17 October 2006

Abstract

The proteomic response of recombinant *Escherichia coli* producing human glucagon-like peptide-1 was analyzed by two-dimensional gel electrophoresis. Protein spots in two-dimensional gel could be identified by using matrix-assisted laser desorption/ionization time-of-flight mass spectrometry and their expression profiles were compared with those of nonproducing cells. Thirty-five intracellular proteins exhibited differential expression levels between the production and control strains. These changes reflected physiological responses to heterologous peptide production in recombinant *E. coli*. Specifically, physiological changes included the down-regulation of proteins involved in the central carbon metabolism, biosynthesis of cellular building blocks and peptides, and up-regulation of cell protection proteins and some sugar transport proteins. This comprehensive analysis would provide useful information for understanding physiological alterations to heterologous peptide production and for designing efficient metabolic engineering strategies for the production of recombinant peptides in *E. coli*.

© 2006 Elsevier B.V. All rights reserved.

Keywords: *Escherichia coli*; Proteomic response; Human glucagon-like peptide-1; Two-dimensional gel electrophoresis

1. Introduction

Human glucagon-like peptide-1 (GLP-1) is a 31-amino acid insulinotropic hormone and plays a physiological role as an incretin hormone responsible for stimulating insulin secretion after meal intake [1]. It also inhibits glucagon secretion and gastric emptying [2]. Since these actions result in lowering postprandial plasma glucose levels in type 2 (noninsulin-dependent) diabetic patients [3], the potential use of GLP-1 for the treatment of this disease has been explored [4]. GLP-1 has been produced by one of the following methods based on *in vitro* chemical syn-

thesis: (a) solid-phase peptide synthesis; (b) liquid-phase peptide synthesis; and (c) enzymatic transacylation [5]. However, chemical synthesis methods show problems such as a low efficiency, high energy demand, and complex processes for reaction, purification and solvent recycle. Recently, the production of GLP-1 by recombinant *Escherichia coli* has been performed because of its dominant position as the first choice of host for the efficient production of valuable recombinant proteins and peptides with high speed, simplicity and well-established production protocols [6]. However, a major disadvantage derived from the intrinsic properties of *E. coli* is the frequent formation of inclusion body, a dense aggregate of misfolded polypeptides [7]. We have studied the biotechnological production of GLP-1 using recombinant *E. coli*. GLP-1 producing *E. coli* cells demonstrated cell growth reduction and inclusion body formation due to the overexpression of GLP-1 [8]. Therefore, an understanding of metabolic and physiological alterations by the production of therapeutic peptides, which are often toxic to cells, is critical for improving the

[☆] This paper is part of a special volume entitled “Analytical Tools for Proteomics”, guest edited by Erich Heftmann.

* Corresponding author at: Department of Agricultural Biotechnology and The BioMAX Institute, Seoul National University, Seoul 151-921, South Korea. Tel.: +82 2 880 4855; fax: +82 2 873 5095.

E-mail address: jhseo94@snu.ac.kr (J.-H. Seo).

productivity of recombinant peptides for academic and industrial purposes. To study the metabolic changes at a whole system level, it is important to consider complex biological systems in their entirety, rather than as a multitude of single cellular compartment. Two-dimensional gel electrophoresis (2-DE) complemented with powerful image analysis software, biological mass spectrometry and database searching engines made it possible to analyze complex protein mixtures extracted from microbial cells [9]. Several groups reported that reasons for physiological changes caused by recombinant protein production could be elucidated by the proteomic analysis of recombinant *E. coli* cells [10,11]. In this study, protein expression profiles of a recombinant *E. coli* producing GLP-1 were analyzed by 2-DE and mass spectrometry, and compared with *E. coli* cells without the target gene in order to gain further insight into global regulatory mechanisms for the expression of GLP-1.

2. Materials and methods

2.1. Chemicals and reagents

Urea, 3-[(3-cholamidopropyl)dimethylammonio]-1-propanesulfonate (CHAPS), dithiothreitol (DTT), immobilized pH gradient (IPG) strip (Immobiline DryStrip, pH 3–10 nonlinear, 180 mm), IPG-buffer (pH 3–10) were obtained from GE Healthcare Bio-Sciences (Piscataway, NJ, USA). Acetone, acetonitrile, 2-propanol, trifluoroacetic acid (TFA) and Coomassie brilliant blue G-250 were purchased from Merck Co. (Darmstadt, Germany). Unless stated otherwise, all reagents and chemicals were purchased from Sigma–Aldrich Co. (St. Louis, MO, USA).

2.2. Bacterial strain and culture condition

A bacterial host strain used in this study was *E. coli* BL21(DE3) transformed with plasmid pK6UbGLP-1. Plasmid pK6UbGLP-1 consisted of the GLP-1 gene fused with the coding region of 6 lysine residues and ubiquitin at the N-terminus under the control of the isopropyl- β -D-thiogalactopyranoside (IPTG) inducible *T7* promoter [8]. Recombinant *E. coli* BL21(DE3) pK6UbGLP-1 was cultured in 100 ml Luria-Bertani (LB) medium (5 g/l yeast extract, 10 g/l tryptone and 10 g/l NaCl) supplemented with 50 μ g/ml of kanamycin at 37 °C. For the expression of GLP-1, IPTG was added into the culture broth at a final concentration of 1 mM when OD₆₀₀ reached to around 0.5. After 2 h induction, the cells were harvested by centrifugation at 8000 \times *g* and 4 °C for 30 min and then stored at –80 °C for further analysis.

2.3. SDS-PAGE and protein quantification

For GLP-1 quantification, cells at the same concentration were harvested by centrifugation at 8000 \times *g* and 4 °C for 5 min and disrupted by sonication. Protein samples were analyzed by sodium dodecyl sulfate polyacrylamide gel electrophoresis (SDS-PAGE) with an 8–16% linear gradient Ready Tris–HCl gel (Bio-Rad). The gels were stained with Coomassie brilliant blue G-250 and the protein bands were normalized and quan-

tified by a GS-700 Calibrated Imaging Densitometer (Bio-Rad, Hercules, CA, USA)

2.4. Sample preparation and electrophoresis

Samples were prepared for 2-DE as described by Choe et al [12] with some modifications. Briefly, pelleted cells were washed four times with low salt washing buffer (3 mM KCl, 1.5 mM KH₂PO₄, 68 mM NaCl, and 9 mM NaH₂PO₄). Cells were subsequently resuspended with lysis solution (9 M urea, 4% (v/v) NP-40 (a nonionic detergent), 1% (w/v) DTT and 2% ampholytes) and subjected to three freeze–thaw cycles. After the final thaw cycle, samples were disrupted by sonication in a 550 Sonic Dismembrator (Fisher Scientific, Pittsburgh, PA, USA) equipped with a cup horn for 5 min on ice and then centrifuged for 30 min at 18,000 \times *g* and 4 °C. Protein concentrations of the resulting supernatants were determined by the Bradford method using bovine serum albumin as a standard. For each sample, 40 μ l of supernatant (approximately 200 μ g protein) was mixed with 60 μ l of a buffer (8 M urea, 4% (w/v) CHAPS, 65 mM DTT in 66.7 mM Tris, pH 8.0) and 300 μ l of rehydration buffer (8 M urea, 2% (w/v) CHAPS, 0.3% (w/v) DTT, 2% ampholytes, 0.002% (w/v) bromophenol blue) for in-gel rehydration. Isoelectric focusing (IEF) and SDS-PAGE were performed as reported previously [12] with modifications given below. IEF was done on a pH 3–10 nonlinear IPG strip (180 mm, GE Healthcare Bio-Sciences) for 78,000 V-h using Protean IEF (Bio-Rad). The IPG strips were then subjected to 12%T SDS-polyacrylamide slab gels (160 mm \times 180 mm \times 1.5 mm) without agarose overlay. The gels were visualized with SYPRO Ruby protein gel stain (Molecular Probes, Eugene, OR, USA) according the manufacturer's instruction.

2.5. 2-DE image analysis

Digitized images of SYPRO Ruby-stained 2-DE gels were acquired by scanning with FLA-3000 (Fujifilm Medical Systems, Stamford, CT, USA) at 50 μ m resolution and 16 bits per pixel. The acquired images of TIFF format were analyzed using Phoretix™ 2D software (Nonlinear Dynamics, Newcastle, UK). Manual editing and removal of artifacts were done after automatic spot detection at default parameters. Gels were analyzed in triplicate.

2.6. Protein identification by mass spectrometry

In-gel digestion was performed essentially as described elsewhere [13]. Briefly, protein spots of interest were excised from stain gels using a commercially available 1.5 mm spot cutter (The Gel Company, San Francisco, CA, USA). The gel pieces were washed in 50% acetonitrile and treated using Investigator ProGest (Genomic Solutions Inc., Ann Arbor, MI, USA) and sequencing-grade modified trypsin (Promega Corporation, Madison, WI, USA). The tryptic digests were desalted and concentrated using C18 ZipTips (Millipore, Bedford, MA, USA) following the manufacturer's protocol. Digest samples were spotted onto stainless steel target plates by a dried droplet

method using α -cyano-4-hydroxycinnamic acid in 50% acetonitrile and 0.1% TFA spiked with 1 mg/ml ammonium phosphate. The sample spots on the plate were analyzed using a 4700 Proteomics Analyzer equipped with matrix assisted laser desorption ionization time-of-flight mass spectrometry (MALDI-TOF MS) (Applied Biosystems, Framingham, MA, USA). Protein identification was based on peptide mass fingerprinting (PMF). Spectra peaks were searched using Mascot via GPS Explorer (version 2.0, Applied Biosystems) using the NCBI database. Protein identification with a confidence interval (C.I.%) score greater than 95% was accepted.

3. Results and discussion

3.1. Growth pattern

E. coli BL21(DE3) pK6UbGLP-1 cells were grown in LB media and compared with the control cells without the GLP-1 gene. *E. coli* BL21(DE3) was grown to OD₆₀₀ of 3.3 at a specific growth rate of 0.45/h while *E. coli* BL21(DE3) pK6UbGLP-1 showed a specific growth rate of 0.15/h in the post-induction period (Fig. 1). A 67% decrease in specific growth rate compared with the control strain seemed to be caused by the overproduction of GLP-1. SDS-PAGE analysis of *E. coli* cells after 2 h induction with 1 mM IPTG exhibited that predominant K6UbGLP-1 bands with around 13 kDa of molecular weight were observed at total and insoluble protein fractions (Fig. 2). Densitometric analysis of the stained gel demonstrated the K6UbGLP-1 fusion peptide accounted for approximately 30% in total cytoplasmic proteins.

3.2. Proteome map

To evaluate the effects of GLP-1 production on physiological changes of *E. coli* cells at a total protein level, comparative analysis of proteome profiles was conducted between the control and GLP-1 producing strains. Each type of *E. coli* cells was analyzed in duplicate to confirm the reproducibility of the culti-

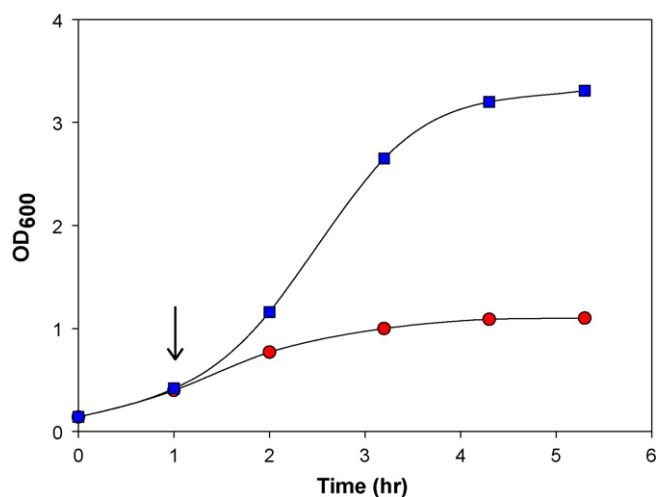


Fig. 1. Time-course growth patterns of *E. coli* BL21(DE3) pK6UbGLP-1 (●) and its parental strain, *E. coli* BL21(DE3) (■) in batch culture. The arrow indicates the addition point of 1 mM IPTG into culture broth.

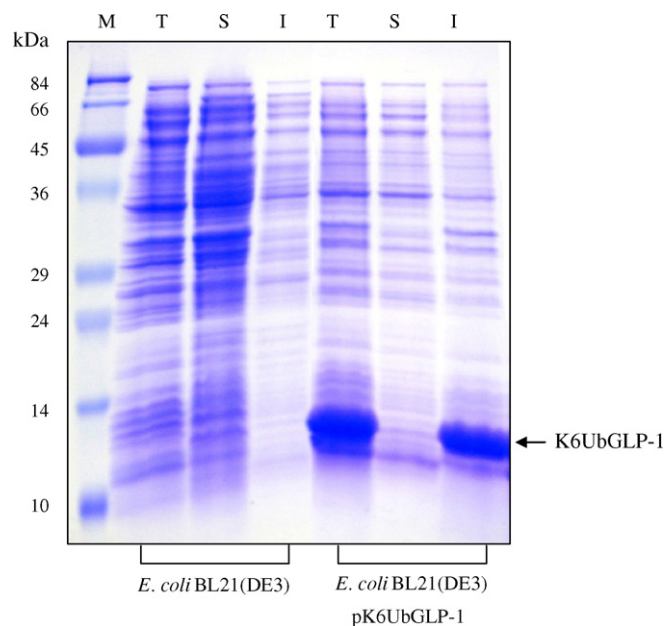


Fig. 2. SDS-PAGE analysis of K6UbGLP-1 expression pattern. Recombinant *E. coli* BL21(DE3) pK6UbGLP-1 and its control *E. coli* BL21(DE3) were grown at 37 °C and K6UbGLP-1 expression was induced by 1 mM IPTG addition. After 2 h of induction, cells were harvested, disrupted and fractionated into total cell lysate (T), soluble fraction (S), and insoluble fraction (I). Lane M denotes a protein molecular weight marker.

vation processes. Each protein sample was analyzed in triplicate by 2-DE with SYPRO Ruby staining of each gel and two of the gel images were subjected to the construction of a reference 2-DE gel image using software Phoretix™ 2D. IEF was performed with nonlinear pH 3–10 IPG strips to analyze a broad range of *E. coli* proteome and to cover the alkaline *pI* of K6UbGLP-1. Several characterized proteins were used as reference spots to calibrate the 2-DE maps.

2-DE protein patterns for each *E. coli* strain were composed of a population of proteins similar to those observed in the previously reported map [14]. For example, molecular chaperones such as GroEL and DnaK, and elongation factor Tu (EF-Tu) encoded by *tufA* were the most abundant proteins in the cells. Tricarboxylic acid cycle enzymes including malate dehydrogenase (Mdh) were also abundant and shown as multiple spots. On average, over 700 spots were visualized on each 2-DE gel image. Of these, 680 most reproducible protein spots were considered for normalization and removal with low confidence. Protein spots showing greater than 18% standard deviation were excluded from analysis. Representative 2-DE profiles of the control and GLP-1 producing *E. coli* were presented in Fig. 3.

3.3. Proteome responses

Table 1 shows the information of identified 89 protein spots by comparing detected spots with the *E. coli* SWISS-2DPAGE database (<http://us.expasy.org/ch2d/publi/ecoli.html>) or by MALDI-TOF MS analysis. A few of the identified proteins (GapA, Pgc, Eno, Mdh, GuaB, DapA, GlnH, GlyA, Crr, FliY and DksA) were observed in multiple spots. A comparison

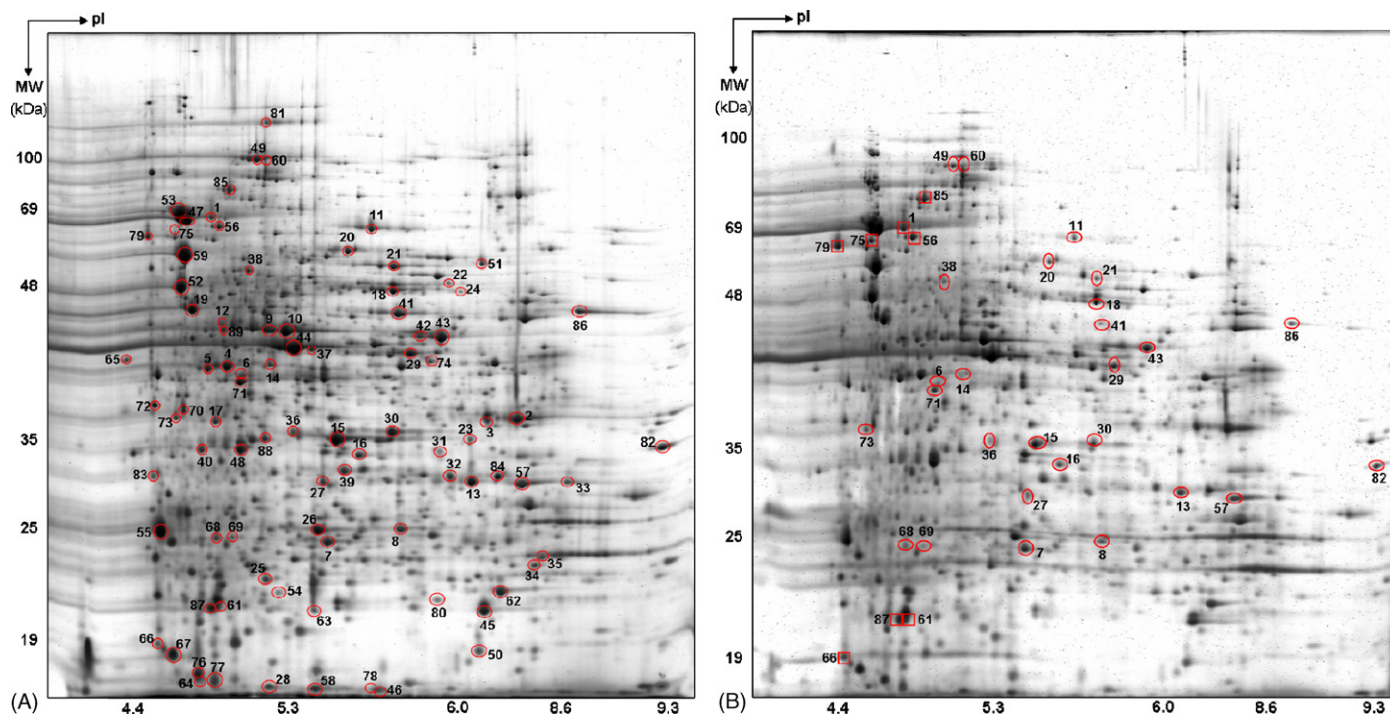


Fig. 3. 2-DE profiles of total proteins expressed in recombinant *E. coli* BL21(DE3) (A) and *E. coli* BL21(DE3) pK6UbGLP-1 (B). Numbered notations refer to representative protein spots listed in Table 1. Rectangles indicate up-regulated proteins and circles present down-regulated proteins upon GLP-1 production (B).

of the control and GLP-1 production proteomes revealed that 35 protein spots consistently exhibited significant changes in abundance (>1.5-fold difference). Twenty-seven protein spots were down-regulated, and 8 up-regulated. Two proteins spot showed on-off changes. On the basis of their identification, protein spots representing proteomic responses to GLP-1 production were divided into several functional classes: central carbon metabolism, biosynthesis and degradation of building blocks, cellular process and regulation.

3.3.1. GLP-1 peptide

There was no spot clearly unique to GLP-1 in the 2-D gel of the GLP-1 producing *E. coli*. Although nonlinear pH 3–10 IPG strips were used to cover the alkaline pI of K6UbGLP-1, any spot of K6UbGLP-1 with a theoretical pI of 9.49 and a theoretical molecular weight of 12,668 was not observed in the 2-DE profiles. K6UbGLP-1 was not detected even when the second dimensional gel electrophoresis with 15%T instead of 12%T was carried out to retain K6UbGLP-1 on the gel for a long time (data not shown). However, the overexpression of K6UbGLP-1 was confirmed by SDS-PAGE analysis (Fig. 2). Reasons for the disappearance of K6UbGLP-1 on 2-D gel were not clear. But commercial IEF strips probably could not cover high alkaline ranges.

3.3.2. Central carbon metabolism

Deregulated metabolic pathways by cellular stresses trigger metabolic imbalance [15]. Changes of metabolic enzyme biosynthesis could alter the balanced metabolite flux and might exert a significant burden on optimal cell growth [16]. Six proteins involved in the central metabolic pathways were repressed

by the production of GLP-1. The dihydrolipotransacylase component of pyruvate dehydrogenase (AceF) catalyzing acetyl-CoA production from pyruvate was up-regulated in the GLP-1 producing cells. However, other glycolytic pathway proteins such as triosephosphate isomerase (TpiA), phosphoglycerate mutase (GpmA) and phosphoglycerate kinase (Pgc) were abundant but down-regulated in the same cell. It was also observed that expression levels of succinate dehydrogenase (SdhA), succinyl-CoA synthetase (SucC and SucD) and malate dehydrogenase (two Mdh isoforms), which are key metabolic enzymes in the tricarboxylic acid (TCA) cycle, were reduced by GLP-1 production. Membrane-bound ATP synthase (AtpA) plays a key role in the free-energy transduction of biological systems. Since the *atpA* deleted *E. coli* mutant was unable to use the proton motive force for ATP synthesis, it grew more slowly than an isogenic wild-type strain [17]. This protein was also down-regulated in the GLP-1 producing *E. coli*. Such a decreased expression level of glycolytic enzymes, TCA cycle-associated enzymes and ATP synthase might lead to a reduced growth rate of the GLP-1 producing *E. coli* relative to the control cell as discussed previously in the growth pattern study.

3.3.3. Building block biosynthesis and degradation

Down-regulation of several amino acid biosynthetic proteins (DapD, CarA, CysK, IlvE and GlnA) was observed in the GLP-1 producing cells. In agreement with a previous study [18], the expression level of cysteine synthase A (CysK) was declined upon GLP-1 production compared with the control. Sharp down-regulation of CTP synthetase (PyrG) and inosine-5'-monophosphate dehydrogenase (GuaB) was also observed in the GLP-1 producing cells. These proteins are involved in

Table 1
List of proteins identified on 2-DE map, as shown in Fig. 3

Spot number	Protein name	Description	pI	MW	Accession number ^a	Fold change ^b	Type of analysis ^c
Central carbon metabolism							
Glycolysis							
1	AceF	Dihydrolipoyltransacetylase component E2 of pyruvate dehydrogenase	5.01	77450	P06959	1.70	MS
2	GapA	Glyceraldehyde 3-phosphate dehydrogenase A	6.70	36386	P06977	1.20	GM
3	GapA	Glyceraldehyde 3-phosphate dehydrogenase A	6.28	36748	P06977	0.72	GM
4	Pgk	Phosphoglycerate kinase	5.02	41974	P11665	1.00	GM
5	Pgk	Phosphoglycerate kinase	5.00	41464	P11665	1.10	MS
6	Pgk	Phosphoglycerate kinase	5.07	41960	P11665	0.48	GM
7	TpiA	Triosephosphate isomerase	4.90	18723	P04790	0.58	GM
8	GpmA	Phosphoglycerate mutase 1	6.27	29204	P31217	0.11	MS
9	Eno	Enolase	5.29	46234	P08324	0.81	GM
10	Eno	Enolase	5.34	46509	P08324	0.93	GM
Tricarboxylic acid cycle							
11	SdhA	Succinate dehydrogenase	5.91	64363	P10444	0.26	MS
12	IcdA	Isocitrate dehydrogenase	5.02	46051	P08200	0.88	GM
13	SucD	Succinyl-CoA synthetase alpha chain	6.16	31613	P07459	0.43	GM
14	SucC	Succinyl-CoA synthetase beta subunit	5.37	41367	P07460	0.34	MS
15	Mdh	Malate dehydrogenase	5.43	35112	P06994	0.31	GM
16	Mdh	Malate dehydrogenase	5.62	33338	P06994	0.55	GM
Pentose phosphate pathway							
17	TalB	Transaldolase B	5.01	35814	P30148	0.89	GM
ATP-proton motive force inter-conversion							
18	AtpA	ATP synthase alpha chain	5.84	53108	P00822	0.63	MS
19	AtpD	ATP synthase beta chain	4.90	47721	P00824	0.98	GM
Building block biosynthesis and degradation							
Nucleotide biosynthesis							
20	PyrG	CTP synthetase	5.63	60336	P08398	0.18	MS
21	GuaB	Inosine-5'-monophosphate dehydrogenase	5.76	56695	P06981	0.12	GM
22	GuaB	Inosine-5'-monophosphate dehydrogenase	6.0	55036	P06981	0.78	GM
23	PyrB	Aspartate carbamoyltransferase catalytic chain	6.13	35321	P00479	1.10	GM
24	UdhA	Soluble pyridine nucleotide transhydrogenase	6.28	49382	P27306	0.91	MS
25	Upp	Uracil phosphoribosyltransferase	5.32	22533	P25532	0.73	GM
26	Adk	Adenylate kinase	5.49	28491	P05082	0.77	GM
Amino acid biosynthesis							
27	DapD	2,3,4,5-Tetrahydropyridine-2-carboxylate N-succinyltransferase	5.56	29873	P03948	0.60	MS
28	AroK	Shikimate kinase I	5.30	17959	P24167	1.00	GM
29	CarA	Carbamoyl-phosphate synthase small chain	5.94	43827	P00907	0.45	MS
30	CysK	Cysteine synthase A	5.81	36027	P11096	0.24	MS
31	DapA	Dihydrodipicolinate synthase	6.00	32916	P05640	1.10	GM
32	DapA	Dihydrodipicolinate synthase	6.10	32361	P05640	1.30	GM
33	YbeJ	Glutamate and aspartate transporter subunit	8.61	33328	P37902	1.10	MS
34	GlnH	Glutamine-binding periplasmic protein precursor	6.93	24504	P10344	0.89	GM
35	GlnH	Glutamine-binding periplasmic protein precursor	7.04	25213	P10344	0.83	GM

Table 1 (Continued)

Spot number	Protein name	Description	pI	MW	Accession number ^a	Fold change ^b	Type of analysis ^c
36	IlvE	Branched-chain amino acid aminotransferase	5.43	35112	P00510	0.47	GM
37	LeuC	3-Isopropylmalate dehydratase	5.42	44439	P30127	0.71	GM
38	GlnA	Glutamine synthetase	5.26	51871	P06711	0.28	MS
Fatty acid biosynthesis							
39	FabI	Enoyl-[acyl-carrier-protein] reductase [NADH]	5.58	27876	P29132	0.83	MS
40	FabD	Malonyl-CoA-[acyl-carrier-protein] transacylase	4.95	32396	P25715	0.71	MS
Amino acid degradation							
41	TnaA	Tryptophan deaminase	5.88	53376	P00913	0.04	MS
42	GlyA	Serine hydroxymethyltransferase	5.94	46142	P00477	0.77	GM
43	GlyA	Serine hydroxymethyltransferase	6.04	45960	P00477	0.61	GM
Protein translation							
44	TufA	Protein chain elongation factor EF-Tu	5.25	44822	P02990	0.94	MS
45	Frr	Ribosome recycling factor	6.16	21725	P16174	0.86	GM
46	RbfA	Ribosome binding factor A	5.79	17433	P09170	1.00	GM
47	RpsA	30S ribosomal protein S1	4.87	67214	P02349	0.98	GM
48	Tsf	Protein chain elongation factor EF-Ts	5.06	33695	P02997	1.30	GM
49	FusA	Protein chain elongation factor EF-G	5.24	77450	P02996	0.40	MS
50	RplI	50S ribosomal subunit protein L9	6.20	19831	P02418	1.20	GM
Glucan biosynthesis							
51	MdoG	Periplasmic glucan biosynthesis protein	6.70	57846	P33136	0.72	MS
Cell processes							
Chaperones							
52	Tig	Trigger factor	4.73	47994	P22257	0.99	MS
53	DnaK	DnaK protein (fragment)	5.00	69646	P04475	1.10	GM
54	DsbA	Thiol:disulfide interchange protein DsbA	5.31	21942	P24991	0.67	GM
55	GrpE	Heat shock protein GrpE	4.68	25542	P09372	0.80	GM
56	HtpG	Molecular chaperone HSP90 family	5.06	65639	P10413	1.60	GM
57	FkpA	Chain A of FKBA type peptidyl-prolyl cis-trans isomerase	6.73	26207	P45523	0.43	MS
58	PpiB	Peptidyl-prolyl cis-trans isomerase B	5.51	17747	P23869	0.69	MS
59	MopA	Cpn60 chaperonin GroEL	4.85	56695	P06139	0.87	GM
60	ClpB	Protein disaggregation chaperone	5.38	73900	P03815	▽	MS
Protection							
61	AhpC	Alkyl hydroperoxide reductase C22 subunit	5.03	20748	P26427	1.70	MS
62	SodA	Superoxide dismutase, Mn	6.44	22920	P00448	0.98	GM
63	SodB	Superoxide dismutase, Fe	5.53	22117	P09157	0.99	GM
64	Tpx	Thiol peroxidase	4.90	18723	P37091	0.68	GM
Transport and binding							
65	Usg	Putative PTS system enzyme II A component	4.38	36372	P08390	0.74	MS
66	Crr	PTS system, glucose-specific IIA component	4.57	20069	P08837	1.80	GM
67	Crr	PTS system, glucose-specific IIA component	4.68	18985	P08837	0.89	MS

Table 1 (Continued)

Spot number	Protein name	Description	pI	MW	Accession number ^a	Fold change ^b	Type of analysis ^c
68	FliY	Cystine transporter subunit	5.01	26213	P39174	0.34	GM
69	FliY	Cystine transporter subunit	5.11	25809	P39174	0.34	MS
70	PotD	Spermidine/putrescine-binding periplasmic protein	4.77	35814	P23861	0.97	GM
71	MalE	Maltose-binding periplasmic protein precursor	5.08	41137	P02928	0.43	MS
72	OmpF	Outer membrane protein F	4.61	36170	P02931	1.00	GM
73	PhoE	Outer membrane pore protein E	4.71	35743	P02932	0.42	GM
74	TolB	Periplasmic protein	5.98	43053	P19935	0.77	GM
75	PtsI	PEP-protein phosphotransferase of PTS system (enzyme I)	4.78	63561	P08839	△	GM
Regulation							
Transcriptional regulation							
76	DksA	DnaK suppressor protein	4.90	18723	P18274	0.89	GM
77	DksA	DnaK suppressor protein	5.01	17853	P18274	0.91	GM
78	Fur	DNA binding transcriptional dual regulator	5.79	17433	P06975	0.68	GM
79	NusA	Transcription termination	4.66	61127	P03003	4.30	MS
80	NusG	Transcription termination factor	6.00	22161	P16921	0.71	MS
Other							
81	CarB	Chain G of carbamoyl phosphate synthetase	5.22	117768	P63737	0.74	MS
82	YdgH	Predicted protein	9.27	33867	P76177	0.53	MS
83	CheZ	Chemotaxis regulator	4.51	28668	P07366	0.68	GM
84	HypB	GTP hydrolase involved in nickel binding into hydrogenases	6.32	32224	P24190	1.00	GM
85	Pnp	Polyribonucleotide phosphorylase/polyadenylase	5.10	83954	P05055	1.60	GM
86	HtrA	Periplasmic serine protease	8.65	49323	P09376	0.51	MS
87	Ppa	Inorganic pyrophosphatase	5.01	21554	P17288	1.60	GM
88	TrxB	Thioredoxin reductase	5.30	34419	P09625	0.99	GM
89	MetK	Methionine adenosyltransferase 1	5.03	44970	P04384	1.10	GM

^a Accession number refers to the SWISSPROT accession code.

^b Fold change of expression level indicates the ratio of a spot density for the GLP-1 producing strain to the control strain. The symbols, △ (on) and ▽ (off), mean on–off changes.

^c MS and GM stand for the mass spectrometry and gel matching, respectively.

the biosynthesis of purine and pyrimidine nucleotides as well as the control of their concentrations. Tryptophan deaminase (TnaA) catalyzing tryptophan degradation to indole, pyruvate and ammonia was one of the most strongly repressed enzymes by GLP-1 production. TnaA synthesis was induced by the presence of L-cysteine produced by CysK [19]. Down-regulated CysK leading to a decrease in L-cysteine concentration probably caused the tight down-regulation of TnaA expression in the GLP-1 synthesizing strain. The GLP-1 producing *E. coli* cells expressed serine hydroxymethyltransferase encoded by *glyA* more lowly than the control strain. This enzyme involved in the biosynthesis of the serine family was repressed when human leptin was produced in *E. coli* [16]. These results showing the limited expression of building block synthesizing enzymes suggested that the production of GLP-1 disturbed a cellular balance in free amino acids, which might lead to the repressed cell growth of GLP-1 producing *E. coli*.

3.3.4. Protein synthesis and folding

Interestingly, protein elongation factor-G (FusA) responsible for protein synthesis was down-regulated, whereas NusA involved in promoting transcriptional termination was strongly up-regulated in the GLP-1 producing *E. coli*. This result might explain a reduction in overall protein synthesis in this recombinant cell. Although the expression levels of heat shock proteins such as DnaK and GroEL increased during the expression of heterologous proteins in *E. coli* [17], the up-regulation of those chaperones were not observed in this study. Coexpression of GroEL/GroES or DnaK/DnaJ/GrpE gave no effect on the soluble expression of K6UbGLP-1 (data not shown). A lower level of peptidyl-prolyl *cis-trans* isomerase (PPIase) chain A (FkpA) was observed in the GLP-1 producing cell. FkpA protein from the *E. coli* periplasm exhibits both PPIase and chaperone activities [20]. Protein disaggregating chaperone (ClpB) showed on–off changes, which was only observed in the control *E.*

coli. ClpB is an Hsp100 protein to mediate the solubilization of aggregated proteins in cooperation with the DnaK chaperone system [21]. Down-regulated FkpA and ClpB might cause the accumulation of K6UbGLP-1 as inclusion body in *E. coli*. The coexpression of molecular chaperones has been used to enhance the cytoplasmic solubility of heterologous proteins in recombinant *E. coli* [22]. Hence, the coexpression of FkpA and/or ClpB with GLP-1 would help the soluble expression of GLP-1. However, HtpG, one of molecular chaperone Hsp90 families, was up-regulated in the GLP-1 producing cell. This could be due to a cellular effort to overcome the imbalance of protein folding components.

3.3.5. Other changes

The amount of an alkyl hydroperoxide reductase subunit (AhpC), which is responsible for DNA protection from oxidative stresses, was higher in the GLP-1 producing cell. It was difficult to quantify the expression level of AhpC due to its comigration with inorganic pyrophosphatase (Ppa). In a previous report, AhpC was required for the protection of cells against high oxidative and/or phosphate-limited stress conditions [23]. Although the underlying reason was unknown, AhpC protein might be needed more to protect the host cells from GLP-1 production stress. Transport and binding proteins (FliY, MalE and PhoE) showed a lower expression level in the GLP-1 producing strain. Meanwhile, bacterial sugar transport-related proteins, glucose-specific enzyme IIA component (Crr) and phosphoenolpyruvate-protein phosphotransferase (PtsI) of the phosphotransferase system, were up-regulated in the same recombinant cell. Since the production and control cultures were performed in LB medium without glucose, more research is necessary to explain why these proteins were induced by GLP-1 production.

4. Conclusion

The differential proteome analysis using 2-DE coupled with MS suggested several key changes in various aspects of cellular physiology including carbon and energy metabolism, building block biosynthesis, protein translation and folding, and cell protection. The additional systematic analyses of transcriptome, metabolome and fluxome are required to achieve a better understanding of global cellular physiology of recombinant *E. coli* in response to GLP-1 production. The integration of proteomic information with physiological properties of a cell could offer

more rational strategies for the genetic modifications of *E. coli* cells with an enhanced protein expression capacity.

Acknowledgements

We are grateful to Leila H. Choe for technical assistance with MALDI-TOF MS analysis. This study was supported by Korea Science and Engineering Foundation (R01-2004-000-10221-0). D. H. Lee and S. K. Kim were supported by Ministry of Education and Human Resources Development through the BK21 program.

References

- [1] M.A. Nauck, J.J. Meier, Regul. Pept. 128 (2005) 135.
- [2] M. Gutniak, C. Ørskov, J.J. Holst, B. Ahren, S. Efendic, N. Engl. J. Med. 326 (1992) 1316.
- [3] M.K. Gutniak, J. Svartberg, P.M. Hellström, J.J. Holst, N. Adner, B. Ahrén, J. Intern. Med. 250 (2001) 81.
- [4] B. Ahrén, Bioessays 20 (1998) 642.
- [5] Z.Z. Zhang, S.S. Yang, H. Dou, J.F. Mao, K.S. Li, Protein Expr. Purif. 36 (2004) 292.
- [6] F. Baneyx, Curr. Opin. Biotechnol. 10 (1999) 411.
- [7] H. Lilie, E. Schwarz, R. Rudolph, Curr. Opin. Biotechnol. 9 (1998) 497.
- [8] S.G. Kim, H.A. Yu, S.Y. Shin, D.H. Kweon, D.O. Kim, W.J. Lee, J.H. Seo, J. Biotechnol., submitted for publication.
- [9] S.R. Pennington, M.R. Wilkins, D.F. Hochstrasser, M.J. Dunn, Trends Cell Biol. 7 (1999) 168.
- [10] K.M. Champion, J.C. Nishihara, I.S. Aldor, G.T. Moreno, D. Andersen, K.L. Stults, M. Vanderlaan, Proteomics 3 (2003) 1365.
- [11] I.S. Aldor, D.C. Krawitz, W. Forrest, C. Chen, J.C. Nishihara, J.C. Joly, K.M. Champion, Appl. Environ. Microbiol. 71 (2005) 1717.
- [12] L.H. Choe, K. Aggarwal, Z. Franck, K.H. Lee, Electrophoresis 26 (2005) 2437.
- [13] E. Finehout, K.H. Lee, Electrophoresis 24 (2003) 3508.
- [14] R.A. Van Bogelen, E.R. Olson, B.L. Wanner, F.C. Neidhardt, J. Bacteriol. 178 (1996) 4344.
- [15] Y.H. Kim, J.S. Park, J.Y. Cho, K.M. Cho, Y.H. Park, J. Lee, Biochem. J. 381 (2004) 823.
- [16] J.K. Kumar, S. Tabor, C.C. Richardson, Proc. Natl. Acad. Sci. 101 (2004) 3759.
- [17] M.J. Han, K.J. Jeong, J.S. Yoo, S.Y. Lee, Appl. Environ. Microbiol. 69 (2003) 5772.
- [18] P.R. Jensen, O. Michelsen, J. Bacteriol. 174 (1992) 7635.
- [19] N. Awano, M. Wada, A. Kohdoh, T. Oikawa, H. Takagi, S. Nakamori, Appl. Microbiol. Biotechnol. 62 (2003) 239.
- [20] J.P. Arie, N. Sassoon, J.M. Betton, Mol. Microbiol. 39 (2001) 199.
- [21] C. Strub, C. Schlieker, B. Bukau, A. Mogk, FEBS Lett. 553 (2003) 125.
- [22] A. De Marco, V. De Marco, J. Biotechnol. 109 (2004) 45.
- [23] P.L. Moreau, F. Gerard, N.W. Lutz, P. Cozzone, Mol. Microbiol. 39 (2001) 1048.